

# *rbk* 基因超表达对类植物乳杆菌 LR-1 生物被膜、黏附特性及代谢谱的调控作用

杨耀<sup>1</sup>, 宋云龙<sup>1</sup>, 陈星<sup>2</sup>, 黎小丽<sup>2</sup>, 龙海祺<sup>2</sup>, 刘蕾<sup>2\*</sup>, 饶瑜<sup>1\*</sup>

1 西华大学 食品与生物工程学院, 四川省食品微生物重点实验室, 四川 成都

2 兰州大学 动物医学与生物安全学院, 动物疫病防控全国重点实验室, 甘肃 兰州

杨耀, 宋云龙, 陈星, 黎小丽, 龙海祺, 刘蕾, 饶瑜. *rbk* 基因超表达对类植物乳杆菌 LR-1 生物被膜、黏附特性及代谢谱的调控作用[J]. 微生物学报, 2025, 65(3): 1241-1265.

YANG Yao, SONG Yunlong, CHEN Xing, LI Xiaoli, LONG Haiqi, LIU Lei, RAO Yu. Overexpression of *rbk* affects the biofilm formation, adhesion, and metabolic profile of *Lactiplantibacillus paraplantarum* LR-1[J]. Acta Microbiologica Sinica, 2025, 65(3): 1241-1265.

**摘要:** 【目的】生物被膜形成和黏附能力是评价益生菌功效的重要指标。然而乳杆菌中特定基因与这些能力的关系尚不清楚。*rbk* 基因编码核糖激酶, 参与核糖代谢, 可能与被膜形成和黏附能力相关。本研究旨在分析 *rbk* 基因超表达对类植物乳杆菌 LR-1 的生物被膜形成和黏附能力的影响, 探讨其对群感及相关基因的调控, 并从代谢谱角度揭示 *rbk* 超表达对菌体的影响机制。【方法】以类植物乳杆菌 LR-1 为目标菌株, 通过穿梭载体 pMG76e 构建 *rbk*-pMG76e-LR-1 重组菌株。通过 qRT-PCR 及酶活试验证实 *rbk* 基因超表达。采用结晶紫染色、细胞黏附试验和 qRT-PCR 分析 *rbk* 超表达对生物被膜形成、黏附能力, 以及 *tuf*、*luxS*、*rpoN* 基因表达的影响; 进一步通过非靶向代谢组学分析 *rbk* 超表达对代谢谱的影响; 最后通过外源添加代谢物验证其对 LR-1 生物被膜形成和黏附能力的影响。【结果】*rbk* 基因超表达显著提升了 LR-1 的生物被膜形成能力(在不同条件下提升 1.55–2.34 倍)和对 HT-29 细胞的黏附能力(约 3.58 倍), 同时显著提升了 *tuf*、*luxS*、*rpoN* 基因表达水平(分别提升 70.30、96.94、45.61 倍)。非靶向代谢组学分析显示, *rbk* 超表达导致 145 种代谢物丰度变化。外源添加代谢物的结果显示, L-脯氨酸、鼠李糖及 NADH 显著提高了 LR-1 生物被膜形成(分别提升 1.27、1.39 和 1.25 倍)和黏附能力(分别提升 1.40、1.41 和 1.52 倍)。【结论】本研究表明 *rbk* 基因可以作为提升乳杆菌生物被膜形成及黏附能力的关键靶点。

**关键词:** 乳杆菌; *rbk* 基因超表达; 生物被膜; 黏附; 非靶向代谢组学

资助项目: 四川省科技计划重点研发项目(2023YFN0058); 四川省自然科学基金(2023NSFSC1203); 甘肃省科技重大专项(23ZDNA007)

This work was supported by the Science and Technology Program Key Research and Development Project of Sichuan Province (2023YFN0058), the Natural Science Foundation of Sichuan Province (2023NSFSC1203), and the Major Science and Technology Project of Gansu Province (23ZDNA007).

\*Corresponding authors. E-mail: LIU Lei, shaning0606@126.com; RAO Yu, ryfish@163.com

Received: 2024-08-28; Accepted: 2024-12-11; Published online: 2025-01-23

# Overexpression of *rbk* affects the biofilm formation, adhesion, and metabolic profile of *Lactiplantibacillus paraplantarum* LR-1

YANG Yao<sup>1</sup>, SONG Yunlong<sup>1</sup>, CHEN Xing<sup>2</sup>, LI Xiaoli<sup>2</sup>, LONG Haiqi<sup>2</sup>, LIU Lei<sup>2\*</sup>, RAO Yu<sup>1\*</sup>

1 Food Microbiology Key Laboratory of Sichuan Province, School of Food and Bioengineering, Xihua University, Chengdu, Sichuan, China

2 State Key Laboratory for Animal Disease Control and Prevention, College of Veterinary Medicine, Lanzhou University, Lanzhou, Gansu, China

**Abstract:** [Objective] Biofilm formation and adhesion are important indicators for evaluating the beneficial effects of probiotics. However, the relationship of specific genes with the biofilm formation and adhesion of *Lactiplantibacillus* remains unclear. The *rbk* gene encodes ribokinase, which is involved in ribose metabolism and may be related to biofilm formation and adhesion. This study aims to analyze the effects of *rbk* overexpression on the biofilm formation and adhesion of *Lactiplantibacillus paraplantarum* LR-1, explore the role of this gene in the regulation of quorum sensing (QS) and expression of related genes, and reveal the influencing mechanism of *rbk* overexpression in bacteria from a metabolic profile perspective. [Methods] *L. paraplantarum* LR-1 was selected as the target strain, and the shuttle vector pMG76e was used to construct the recombinant strain *rbk*-pMG76e-LR-1. The overexpression of *rbk* was confirmed by qRT-PCR and the enzyme activity assay. Crystal violet staining, cell adhesion assay, and qRT-PCR were employed to evaluate the effects of *rbk* overexpression on biofilm formation, adhesion, and expression of *tuf*, *luxS*, and *rpoN*. Furthermore, untargeted metabolomics analysis was conducted to assess the effect of *rbk* overexpression on the metabolic profile. Finally, the effect on the biofilm formation and adhesion of LR-1 was verified by exogenous addition of metabolites. [Results] The overexpression of *rbk* increased the biofilm formation of LR-1 and the adhesion to HT-29 cells by 1.55–2.34 folds and 3.58 folds, respectively. Moreover, the overexpression of *rbk* up-regulated the expression levels of *tuf*, *luxS*, and *rpoN* by 70.30, 96.94, and 45.61 folds, respectively. The untargeted metabolomics analysis revealed that *rbk* overexpression led to changes in the abundance of 145 metabolites. Finally, the exogenous addition of L-proline, rhamnose, and nicotinamide adenine dinucleotide (NADH) increased the biofilm formation of LR-1 by 1.27, 1.39, and 1.25 folds and the adhesion by 1.40, 1.41, and 1.52 folds, respectively. [Conclusion] This study demonstrates that *rbk* can serve as a key target for enhancing the biofilm formation and adhesion of *Lactiplantibacillus*.

**Keywords:** *Lactiplantibacillus*; *rbk* overexpression; biofilm; adhesion; untargeted metabolomics

Lactic acid bacteria (LAB), especially the species of genus *Lactobacillus*, have recently received attention because of their generally recognized as safe (GRAS) status and their potential health-promoting effects as probiotics<sup>[1]</sup>. As probiotics, *Lactobacillus* plays an important role in maintaining gut microbiota balance, promoting intestinal health, preventing diarrhea and alleviating colitis symptoms, etc<sup>[2]</sup>. An important criterion for probiotics is their ability to withstand unfavorable conditions in the gastrointestinal tract and their capacity to adhere and colonize the intestinal mucosa<sup>[1]</sup>. In natural environments, many bacteria including LAB can form biofilms to resist adverse external conditions. And in the host's intestine, the formation of biofilms on the intestinal mucosal epithelial cells allows bacteria to better withstand the cleansing actions caused by intestinal peristalsis and the flushing of intestinal fluids<sup>[3]</sup>. Currently, one of the latest probiotic formulation technologies involves preparing probiotics in the form of biofilms to withstand environmental stresses during production and digestion<sup>[4]</sup>. Therefore, exploring the key genes associated with biofilm formation in probiotic LAB is of significant importance. Currently, research into the molecular mechanisms of biofilm formation in pathogenic bacteria has progressed significantly; however, studies related to *Lactobacillus* are still quite limited. It is still very necessary to explore the relationships between specific genes in *Lactobacillus* and biofilm formation.

Our previous research has identified a series of genes that may be associated with quorum sensing (QS) and biofilm formation in *Lactobacillus*, including the *rbk* gene. The enzyme encoded by the

*rbk* gene is ribokinase, which has the fundamental physiological function of degrading D-ribose and ATP to produce ribose-5-phosphate and ADP. The substrate, ribose, has no toxic effects and has structural similarity with autoinducer 2 (AI-2). It is the signal molecules of the *LuxS/AI-2* quorum sensing system<sup>[5]</sup>. This structural similarity allows the AI-2 receptor to bind with ribose, meaning that the presence of ribose could competitively bind to the AI-2 receptor, thereby blocking the downstream signaling pathways regulating QS-related physiological behaviors, such as biofilm formation<sup>[6]</sup>. In addition, ribose, a common monosaccharide in the environment, could present a carbon source for gastrointestinal microbiota components<sup>[7]</sup>. And ribose could be used to synthesize nucleotides and amino acids (histidine and tryptophan) and is also an essential energy source<sup>[8]</sup>. Among them, purine nucleotide synthesis is related to biofilm formation in *Lactobacillus*<sup>[9]</sup>, and L-histidine metabolism has been reported to trigger the biofilm formation of *A. baumannii*<sup>[10]</sup>. Therefore, changes in ribose metabolism can influence bacterial physiological behavior from multiple dimensions, potentially including the physiological behaviors of individual cells as well as those of cell populations, such as biofilm formation and adhesion colonization.

This study selects *Lactiplantibacillus paraplantarum* LR-1 as the research subject, which is originally isolated from fermented vegetables. This strain has probiotic properties, such as alleviating colitis<sup>[11]</sup>. In this study, the *rbk* gene was recombined with the pMG76e shuttle vector and then introduced into the *L. paraplantarum* LR-1 strain. The effects of the introduction and

overexpression of this gene on the growth and biofilm formation were measured, as well as its influence on the expression of biofilm and QS-related genes *tuf*, *rpoN* and *luxS*. Additionally, the overall metabolic impact of the introduction and overexpression of the *rbk* gene on the bacterial cells was further assessed through untargeted metabolomics. This study is valuable for understanding the relationship between the *rbk* gene and the physiological behaviors and metabolism of *Lactobacillus*.

## 1 Materials and Methods

### 1.1 Bacterial strains, cells, and culture conditions

The strain used in this experiment was *L. paraplantarum* LR-1 (CICC 24809), isolated from Sichuan pickles. The strain was cultured in de Man-Rogosa-Sharpe (MRS) broth (Beijing Land Bridge Technology Co., Ltd.) or MRS-Agar under aerobic conditions at a temperature of 37 °C. *Escherichia coli* (*E. coli*) DH5 $\alpha$  (TaKaRa Biotechnology (Dalian) Co., Ltd.) was cultured in Lennox broth (LB) or LB agar under aerobic conditions at a temperature of 37 °C. *E. coli* DH5 $\alpha$  containing pMG76e vector and *L. paraplantarum* LR-1 containing pMG76e vector were cultured in LB medium containing 200  $\mu$ g/mL of erythromycin and in MRS medium containing 3  $\mu$ g/mL of erythromycin, respectively.

The HT-29 cells were purchased from the American Type Culture Collection (ATCC). Cells were cultured in Dulbecco's Modified Eagle Medium (DMEM, Amresco) containing 10% (*V/V*) fetal bovine serum (Zhejiang TianHang Biotechnology Co., Ltd.), 1% dual antibiotics (penicillin (100 IU/mL,

ThermoFisher Scientific) and streptomycin (100  $\mu$ g/mL, ThermoFisher Scientific)) at 37 °C in an atmosphere of 5% CO<sub>2</sub>/95% air at constant humidity.

### 1.2 Construction of plasmids and bacterial strains

The chromosomal DNA of *L. paraplantarum* LR-1 was extracted using a TIANamp Bacteria DNA Kit (Tiangen Biotech (Beijing) Co., Ltd.) according to the manufacturer's instructions. Using the genomic DNA as template, the *rbk* gene was amplified by PCR with primers containing *Xba* I and *Xho* I restriction sites (Table 1). The PCR-amplified *rbk* gene fragment was ligated with the pMD-18T vector (TaKaRa Biotechnology (Dalian) Co., Ltd.) and then introduced into the competent *E. coli* DH5 $\alpha$  cells (TaKaRa Bio technology (Dalian) Co., Ltd.) for amplification. Next, the *rbk*-pMD-18T recombinant plasmid was double-digested with *Xba* I and *Xho* I (ThermoFisher Scientific) to obtain the *rbk* gene fragment, which was then ligated with the similarly double-digested pMG76e using a Rapid DNA Ligation Kit (ThermoFisher Scientific) to construct the *rbk*-pMG76e recombinant vector.

The competent cells of *L. paraplantarum* LR-1 were prepared as follows. Briefly, the LR-1 strain was inoculated into MRSS medium (MRS medium containing 0.3 mol/L sucrose) containing 1% glycine and cultured until the OD<sub>600</sub> reached between 0.4 and 0.6. A 10 mL aliquot of the culture was then centrifuged at 6 000 r/min for 8 min at 4 °C to collect the cells. The pellet was resuspended in 2 mL of washing buffer (0.3 mol/L sucrose with 0.1 mol/L MgCl<sub>2</sub>) and centrifuged again at 6 000 r/min

Table 1 Primers for PCR in this study

Primers	Sequences (5'→3')
<i>rbk-1-F</i>	TGCTCTAGAATGAATACGGTAACAGTG
<i>rbk-1-R</i>	CCGCTCGAG TTATTTACCCTCCGCGGC

for 8 min at 4 °C. Finally, the cells were resuspended in 2 mL of 30% PEG-1500 and centrifuged at 6 000 r/min for 10 min. The final pellet was resuspended in 200 µL of 30% PEG-1500 and kept on ice for further use. The recombinant plasmid *rbk*-pMG76e was introduced into the competent LR-1 cells by electroporation under the conditions of 1.5 kV and 400 Ω. After the electroporation, the cells were allowed to rest on ice for 5 min before adding 1 mL of MRSSM medium (MRS containing 0.3 mol/L sucrose and 0.1 mol/L MgCl<sub>2</sub>) and incubating at 37 °C for 2 h. The cells were then spread on MRS plates containing 3 µg/mL of erythromycin and incubated at 37 °C for 36–48 h. Positive clones were selected and identified by PCR, confirming the presence of the *rbk*-pMG76e recombinant strain.

### 1.3 Real-time quantitative PCR (qRT-PCR)

The strain containing the empty vector pMG76e (pMG76e-LR-1), the recombinant strain with the plasmid *rbk*-pMG76e (*rbk*-pMG76e-LR-1), and the wild-type strain LR-1 were cultured overnight at 37 °C in MRS medium. Total RNA was extracted using TRIzol Agent (ThermoFisher Scientific) according to the manufacturer's instructions. The RNA quality was assessed using the  $A_{260}/A_{280}$  and  $A_{260}/A_{230}$  ratios. The extracted RNA was converted into cDNA using a TUREscript 1st Strand cDNA Synthesis Kit (Aidlab Biotechnologies Co., Ltd.). The expression levels of the genes *rbk*, *tuf*, *luxS* and

*rpoN* were determined using quantitative reverse transcription polymerase chain reaction (qRT-PCR). The 16S rRNA gene was used as the reference gene. The primers for the relevant genes (Table 2) were designed using the Primer 3 input online tool (<https://primer3.ut.ee/>). The relative expression levels of the genes were calculated using the  $2^{-\Delta\Delta C_t}$  method, as described by Livak and Schmittgen<sup>[12]</sup>.

### 1.4 Ribokinase activity assay

The strains *rbk*-pMG76e-LR-1, pMG76e-LR-1 and the wild-type LR-1 were cultured in MRS without erythromycin for 8 h. The cells were centrifuged at 5 000×g at 4 °C for 5 min and washed three folds with PBS. The viable cell counts of the three strains were determined using the plate counting method and standardized. The bacterial cells were then disrupted by ultrasound at 4 °C for 20 min (4 s work+6 s break for 120 cycles). The lysed cells were centrifuged at 5 000×g at 4 °C for 20 min, and the supernatant was collected.

Ribokinase activity was measured using a Ribokinase (RBKS) Enzyme-linked Immunoassay Kit (Shanghai Jingkang Bioengineering Co., Ltd.) according to the manufacturer's instructions.

Table 2 Primers for qRT-PCR in this study

Primers	Sequences (5'→3')
<i>rbk-2-F</i>	AGGTCCCCGCTGAACCTTTTA
<i>rbk-2-R</i>	CACCAGCTGACGTTGTATCG
<i>tuf-F</i>	CGCAACTGATGGTCCTATGC
<i>tuf-R</i>	CGCTGAACCACGGATAACAG
<i>luxS-F</i>	TGATACAGCGGGCTTACACA
<i>luxS-R</i>	CTCCCACTTAGCTGGACCA
<i>rpoN-F</i>	CCAAGCAATTCGGGACTACG
<i>rpoN-R</i>	TTTCTTCTGCCCGGAGAACT
<i>16S RNA-F</i>	CAACGAGCGCAACCCTTATT
<i>16S RNA-R</i>	GCAGCCTACAATCCGAAGCTG

Samples were added into microtiter plate coated with purified ribokinase antibodies, and then combined with horseradish peroxidase (HRP)-labeled ribokinase antibodies to form an antibody-antigen-enzyme-labeled antibody complex, which is washed and then added into Tetramethylbenzidine (TMB) to initiate color development. Under the catalytic action of HRP enzyme, TMB will be converted into blue, and finally into yellow under the action of acid. The intensity of the color is directly proportional to the ribokinase concentration in the samples. And the ribokinase activity was quantified by measuring the absorbance at 450 nm and referencing a standard curve.

### 1.5 Growth curves

The recombinant *rbk*-pMG76e-LR-1, pMG76e-LR-1 strains and the wild-type LR-1 strain were cultured in MRS without erythromycin. The cell densities were determined at 3, 6, 9, 12, 15, 18, 21, 24, 27, 30, 33, and 36 h by measuring the  $OD_{600}$  using a UV-1800 Spectrophotometer (Shimadzu).

### 1.6 Biofilm formation assay

The biofilm-forming ability of the strains *rbk*-pMG76e-LR-1, pMG76e-LR-1 and the wild-type LR-1 was determined using the crystal violet (CV) staining method<sup>[6]</sup>. In brief, the initial  $OD_{600}$  value of the three strains was adjusted to 0.1, and then they were inoculated into a 96-well cell culture plate (Corning Incorporated). After incubating at 37 °C for 48 h, the plate was gently washed with PBS, followed by staining with 0.1% CV for 30 min. The plate was then washed with sterile water and allowed to air dry. Finally, 100 µL of 95% ethanol was added to each well to dissolve the CV, and the absorbance at 595 nm was measured

using a Synergy 2 Microplate Reader (Winooski). The strains *rbk*-pMG76e-LR-1, pMG76e-LR-1 and the wild-type LR-1 were cultured in MRS at pH 4.0, with 0.2% bile salt and 8.0% (*W/V*) NaCl at 37 °C for 48 h to form biofilms, and the biofilms were detected as described above.

### 1.7 Adhesion assay

HT-29 cells were cultured in a 24-well plates (Corning Incorporated) until a monolayer was formed, with approximately  $2.5 \times 10^5$  cells per well. The cells were then washed twice with PBS (pH 7.2). At the same time, after overnight culture, the strains *rbk*-pMG76e-LR-1, pMG76e-LR-1, and the wild-type LR-1 were collected by centrifugation ( $5\ 000 \times g$ , 4 °C, 10 min), washed twice with PBS, and resuspended in DMEM at a final concentration of  $1 \times 10^8$  CFU/mL. Subsequently, 100 µL of the bacterial suspension was added to each well of the 24-well plate to co-culture with HT-29 cells, at a bacteria-to-cell ratio of  $10^7:2.5 \times 10^5$ , and incubated at 37 °C for 1.5 h. After the incubation, the plate was washed twice with PBS to remove non-adherent bacteria. Then, Triton X-100 was used to dissociate the adhered bacteria. The adhesion rate was calculated using the formula (1)<sup>[13]</sup>.

$$\text{Adhesion ratio} = \frac{\text{Bacterial counts after adhesion}}{\text{Bacterial counts before adhesion}} \times 100\% \quad (1)$$

### 1.8 Untargeted metabolomics analysis

#### 1.8.1 Sample extraction

The *rbk*-pMG76e-LR-1 and pMG76e-LR-1 strains were cultured in MRS without erythromycin for 8 h. Afterwards, the cells were collected by centrifugation at  $5\ 000 \times g$  for 5 min at 4 °C. Then, 60 mg of each sample was resuspended in 200 µL of water and mixed thoroughly for 60 s. Then, 800 µL

of extraction solvent (methanol:acetonitrile=1:1) was added, and the mixture was homogenized for 60 s. This was followed by ultrasound treatment in ice-water for 30 min, which was repeated twice. The samples were then stored at  $-20\text{ }^{\circ}\text{C}$  for 1 h to allow protein precipitation, followed by centrifugation at  $12\ 000\times g$  for 20 min at  $4\text{ }^{\circ}\text{C}$ . The supernatant was dried using a vacuum concentrator and subsequently stored at  $-80\text{ }^{\circ}\text{C}$ .

### 1.8.2 Mass spectrometry

The analyses were performed using UHPLC (Agilent Technologies) coupled with a quadrupole time-of-flight (Sciex) at Shanghai Applied Protein Technology Co., Ltd. For HILIC separation, the samples were analyzed using a  $2.1\text{ mm}\times 100\text{ mm}$  ACQUITY UPLC BEH  $1.7\text{ }\mu\text{m}$  column (Waters Corporation). In both ESI positive and negative modes, the mobile phase consisted of A: 25 mmol/L ammonium acetate and 25 mmol/L ammonium hydroxide in water, and B: acetonitrile. For RPLC separation, a  $2.1\text{ mm}\times 100\text{ mm}$  ACQUITY UPLC HSS T3  $1.8\text{ }\mu\text{m}$  column (Waters Corporation) was utilized. In ESI positive mode, the mobile phase comprised A: water with 0.1% formic acid and B: acetonitrile with 0.1% formic acid. In ESI negative mode, the mobile phase consisted of A: 0.5 mmol/L ammonium fluoride in water and B: acetonitrile. For MS/MS analysis, the ESI source conditions were set as follows: Ion Source Gas1 (Gas1) as 60, Ion Source Gas2 (Gas2) as 60, curtain gas (CUR) as 30, source temperature:  $600\text{ }^{\circ}\text{C}$ , and IonSpray Voltage Floating (ISVF) $\pm 5\ 500\text{ V}$ .

### 1.8.3 Data analysis

The raw MS data (wiff. scan files) were converted to MzXML files using ProteoWizard MS

Convert v3.0.6458 before importing into freely available XCMS software. After normalizing total peak intensity, the processed data were uploaded into SIMCA-P (v14.1), where they underwent multivariate data analysis, including Pareto-scaled principal component analysis (PCA), partial least-squares discriminant analysis (PLS-DA), and orthogonal PLS-DA (OPLS-DA). Metabolites with variable importance for the projection (VIP) value $>1$  were further analyzed for significance, with a threshold of  $P<0.05$  was considered statistically significant.

### 1.8.4 Bioinformatic analysis

The metabolites were matched against the online Kyoto encyclopedia of genes and genomes (KEGG) database (<http://geneontology.org/>). KEGG pathway enrichment analyses were conducted using Fisher's exact test, with pathways yielding a  $P$ -value less than 0.05 considered significant. The relative expression data of the analyzed metabolites were utilized to perform hierarchical clustering analysis using Cluster 3.0 (<http://bonsai.hgc.jp/~mdehoon/software/cluster/software.htm>).

## 1.9 Evaluation of the effects of exogenous metabolites on biofilm formation and adhesion of LR-1

Based on the metabolomic analysis results, this experiment selected 8 metabolites related to bacterial biofilm formation and adhesion. These include L-histidine, L-proline, L-arginine, L-serine (Solarbio), Rhamnose, N-acetyl-D-lactosamine, NADH (Shandong Sparkjade Biotechnology Co., Ltd.), and D-mannose-6-phosphate (Rhawn). Solutions of these metabolites were prepared at a concentration of 50 mg/mL, and the pH was adjusted to neutral.

The CV staining method was used to assess

the impact of the aforementioned 8 metabolites on the biofilm formation of LR-1. Briefly, the bacterial suspension was adjusted to an  $OD_{600}$  of 0.1 and inoculated into 96-well cell culture plates with 100  $\mu$ L per well. Subsequently, 100  $\mu$ L of the metabolites solution diluted with MRS broth was added, resulting in a final concentration of 100 mg/mL. After incubation at 37 °C for 48 h, the biofilms were detected as aforementioned in section 1.6.

The adhesion experiment set up two treatment methods: one involved culturing LR-1 with exogenous metabolites before extracting the bacterial cells and co-culturing them with HT-29 cells, referred to as the met-LR-1-post-LR-1 group. The other method involved simultaneous co-culturing of exogenous metabolites, LR-1, and HT-29 cells, referred to as the met-LR-1-HT-29 group. The specific procedure for the met-LR-1-post-LR-1 group was as follows: 8 exogenous metabolites were added to fresh LR-1 bacterial suspension to achieve a final concentration of 10 mg/mL, with a bacterial concentration of  $10^8$  CFU/mL. After incubating at 37 °C for 9 h, the bacteria were collected by centrifugation, and the bacterial suspension was adjusted to a concentration of  $10^8$  CFU/mL before co-culturing with HT-29 cells in 24-well plates, maintaining a bacteria to cell ratio of  $10^7:2.5 \times 10^5$ . For the met-LR-1-HT-29 group, the procedure involved simultaneous co-culturing of bacteria, cells, and exogenous metabolites, with the final concentration of metabolites also set at 10 mg/mL and a bacteria to cell ratio of  $10^7:2.5 \times 10^5$ . The co-culturing time was 1.5 h, after which the adhesion rate was calculated, following the same method as described in section 1.7.

## 1.10 Statistical analysis

Significant differences were determined using analysis of variance (ANOVA) in *R* (v4.1.1). Data are presented as mean $\pm$ standard deviation (SD). *P*-values less than 0.05 were considered significant, with \*\*\* representing  $P < 0.001$ , \*\* representing  $P < 0.01$ , \* representing  $P < 0.05$ , and ns indicating no significance. Each experiment was conducted in triplicate, with each test involving at least three separate measurements. In the case of untargeted metabolomics analysis, six samples were analyzed. The relationships between significantly different metabolites and the phenotype of strains were calculated using the Pearson correlation coefficient with the OmicShare tools, a free online platform for data analysis (<http://www.omicshare.com/tools>). Cytoscape (v3.8.2) was employed to visualize the interaction networks among the significantly different metabolites and the phenotype of the strains.

## 2 Results and Discussion

### 2.1 The successful construction of the recombinant strain *rbk*-pMG76e-LR-1 with overexpression of the *rbk* gene

The PCR identification results of strains containing the recombinant plasmids *rbk*-pMG76e and pMG76e are shown in Figure 1A–1B. The results indicate that the plasmids *rbk*-pMG76e and pMG76e were successfully introduced into LR-1 bacterial cells. Furthermore, the qRT-PCR results indicated that, as shown in Figure 1C, the introduction of plasmid pMG76e did not affect the expression of the *rbk* gene. In contrast, the introduction of the recombinant plasmid *rbk*-pMG76e significantly increased the expression of the *rbk*

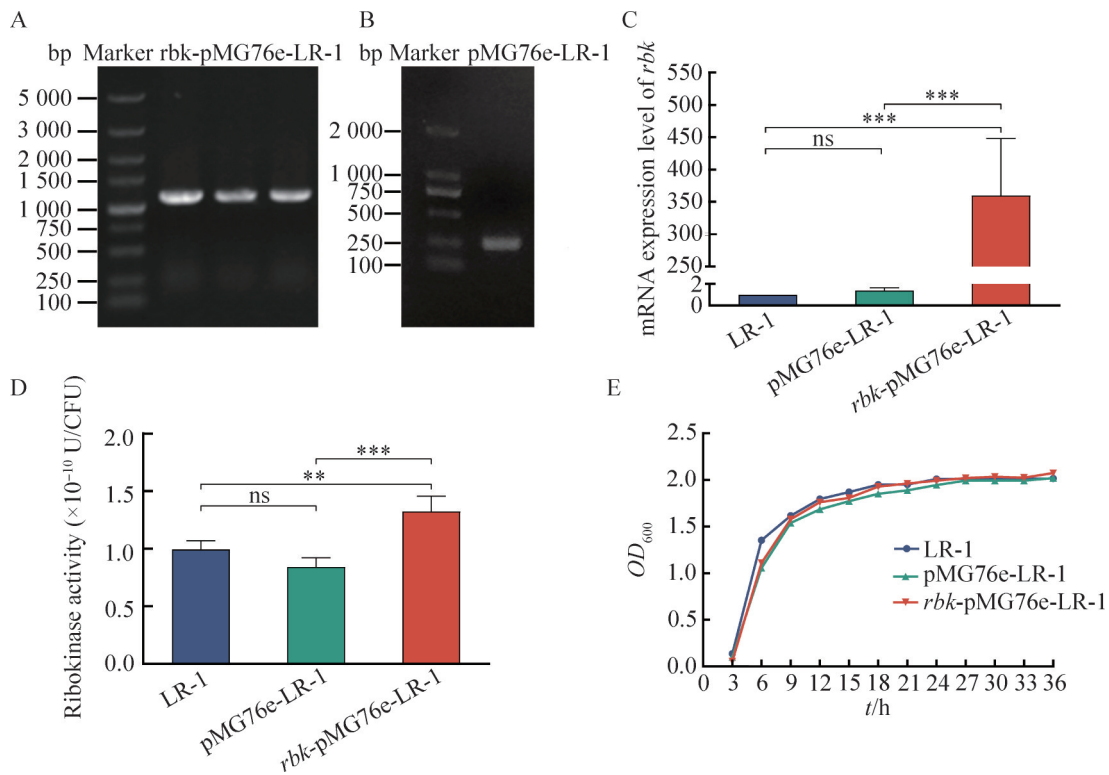


Figure 1 The *rbk* gene was successfully overexpressed in LR-1. PCR validation of the *rbk*-pMG76e-LR-1 (A) and pMG76e-LR-1 (B) recombinant strains. Detection of the *rbk* gene transcriptional levels (C), ribokinase activity (D) and growth curves (E) in LR-1 (wild-type), pMG76e-LR-1, and *rbk*-pMG76e-LR-1 strains. The data obtained from three separate experiments are presented as mean±SD. \*\*\*:  $P<0.001$ ; \*\*:  $P<0.01$ ; ns: No significant.

gene in LR-1, with an enhancement of 359.81 folds ( $P<0.001$ ). The ribokinase enzyme activity assay similarly indicated that the introduction of the pMG76e plasmid did not affect the ribokinase activity of the LR-1 bacterial cells. However, the introduction of the recombinant plasmid *rbk*-pMG76e resulted in a 1.33 folds increase in ribokinase activity in the bacterial cells (Figure 1D,  $P<0.01$ ). The growth experiments, as shown in Figure 1E, showed that the introduction of both pMG76e and *rbk*-pMG76e did not significantly affect the growth of LR-1.

The *rbk* gene encodes ribokinase and is

involved in the phosphorylation metabolic process of ribose<sup>[6,14]</sup>. When ribose is present in the external environment, the *rbk* gene responds accordingly<sup>[6]</sup>. This study demonstrates that the expression level of the intracellular *rbk* gene and the corresponding enzyme activity can be enhanced through the introduction of an exogenous recombinant plasmid. Additionally, although the introduction of plasmids pMG76e and *rbk*-pMG76e did not affect the maximum growth concentration of LR-1, it slightly influenced the early growth rate of the cells. This may be attributed to damage caused during the preparation of competent cells or the electroporation

process, which could affect intracellular metabolism. However, these effects are likely to be mitigated as bacterial growth progresses.

## 2.2 The overexpression of the *rbk* gene enhanced the biofilm formation and adhesion capabilities of the LR-1 strain

The biofilm formation results are illustrated in Figure 2A–2D. The introduction of pMG76e did not affect the biofilm formation of LR-1. However, the overexpression of the *rbk* gene significantly enhanced the biofilm formation ability of LR-1. Under normal culture conditions, the biofilm formation of *rbk*-pMG76e-LR-1 increased to approximately 1.55 folds (Figure 2A). The enhancement of biofilm formation was even more pronounced under stress conditions. Under stress conditions of pH 4.0, 0.2% bile salt, and high salt, the overexpression of *rbk* increased the biofilm formation of the LR-1

strain to about 1.88, 2.34 and 1.62 folds, respectively. Additionally, the introduction of the pMG76e plasmid did not affect the adhesion ability of the LR-1 strain, while the introduction of the *rbk*-pMG76e plasmid increased the strain's adhesion to HT-29 cells to approximately 3.58 folds (Figure 2E).

Bacteria in a biofilm state possess a stronger ability to resist adverse external environments<sup>[4,6,14]</sup>. Therefore, developing biofilm-forming probiotics is currently one of the important research directions for next-generation probiotic formulations<sup>[15-16]</sup>. This study suggests that the *rbk* gene can serve as a key target for enhancing the expression level to improve the biofilm formation ability of *Lactobacillus*. Additionally, the formation of biofilms by bacteria is a response mechanism to adverse external environments<sup>[3]</sup>. The results of this study indicate that enhancing the expression of the *rbk* gene can

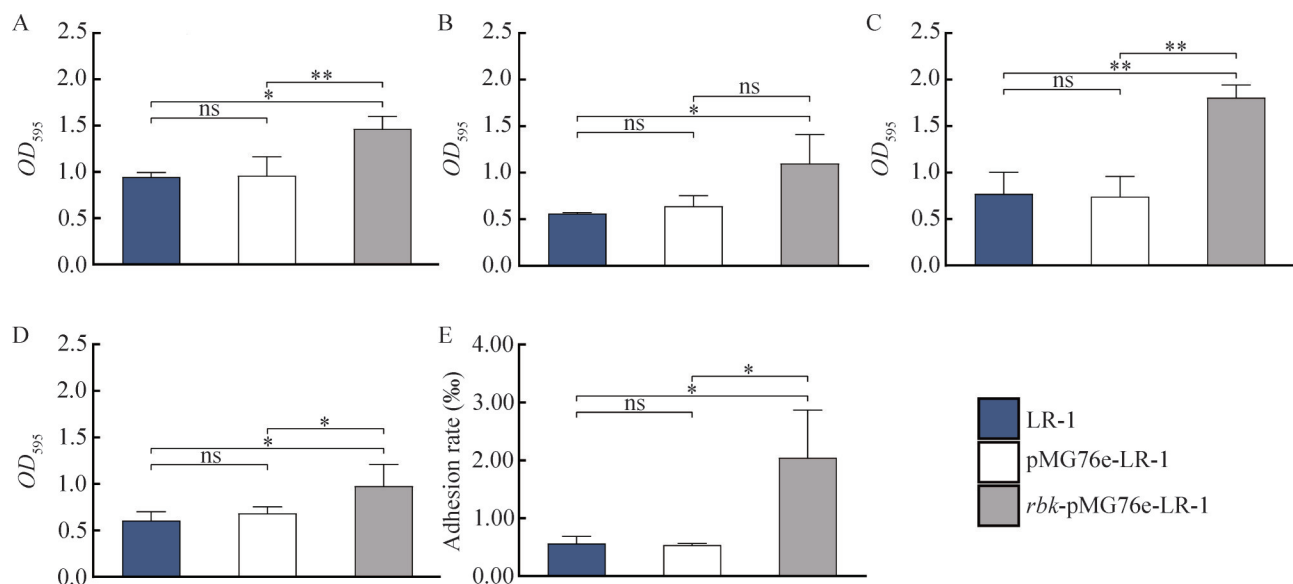


Figure 2 The overexpression of the *rbk* gene enhanced the biofilm formation and adhesion abilities of the LR-1 strain. The biofilm formation of LR-1, pMG76e-LR-1, and *rbk*-pMG76e-LR-1 in MRS (A), MRS with pH 4.0 (B), MRS with 0.2% (*W/V*) bile salt (C), and MRS with 8.0% (*W/V*) NaCl (D). The adhesion of the three strains to HT-29 cells (E). The data obtained from three separate experiments are presented as mean±SD. \*\*:  $P < 0.01$ ; \*:  $P < 0.05$ ; ns: No significant.

effectively increase the biofilm formation ability of *Lactobacillus* under common stress environments experienced probiotics. Furthermore, adhesion ability is one of the most critical indicators for evaluating the health benefits of probiotics, which is often positively correlated with biofilm formation ability<sup>[3]</sup>. This study demonstrates that the *rbk* gene can be a target for enhancing the adhesion ability of *Lactobacillus*. Although research on the relationship between the *rbk* gene and bacterial physiological phenotypes, especially probiotics, is still lacking, this study highlights *rbk* as a potential target for enhancing the probiotic effects of *Lactobacillus*, representing a significant addition to related research.

### 2.3 The overexpression of the *rbk* gene upregulated the expression of *tuf*, *luxS* and *rpoN* genes in the LR-1 strain

Our previous research has identified the *tuf*, *luxS* and *rpoN* genes as three genes closely related to biofilm formation in *Lactobacillus*<sup>[6,13]</sup>. In this study, the effect of *rbk* gene overexpression on the expression levels of these three genes is shown in Figure 3. The results indicate that the introduction of the pMG76e plasmid had no significant impact on the expression levels of *tuf*, *luxS* and *rpoN* in the LR-1 strain. However, the introduction of the *rbk*-pMG76e recombinant plasmid significantly increased the expression levels of the aforementioned three genes. Overexpression of the *rbk* gene led to an approximate upregulation of the expression levels of *tuf*, *luxS*, and *rpoN* to about 70.30, 96.94 and 45.61 folds, respectively.

The *tuf*, *luxS* and *rpoN* genes are three genes that we previously identified through high-throughput screening and preliminary validation to have a

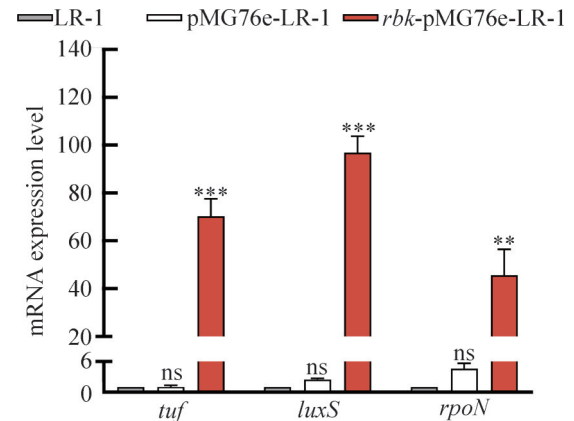


Figure 3 The overexpression of *rbk* in LR-1 upregulates the expression of *tuf*, *luxS*, and *rpoN* genes. The data obtained from three separate experiments are presented as mean±SD. \*\*\*:  $P < 0.001$ ; \*\*:  $P < 0.01$ ; ns: No significant.

significant positive correlation with biofilm formation in *Lactobacillus*<sup>[6]</sup>. The *tuf* gene encodes the elongation factor EF-Tu, which is a protein responsible for peptide chain elongation and protein folding, and it is also associated with stress resistance<sup>[17]</sup>. Additionally, EF-Tu has been found to be an adhesion-related factor in *Lactobacillus acidophilus*, *Lactobacillus plantarum*, and *Lactobacillus johnsonii*<sup>[18-19]</sup>. The *luxS* gene encodes the LuxS protein, which is involved in methionine metabolism. In this process, LuxS converts S-adenosylhomocysteine (SAH) into S-ribosylhomocysteine (SRH) while generating a byproduct<sup>[20]</sup>. This byproduct is the signaling molecule AI-2, which is involved in QS of both Gram-positive and Gram-negative bacteria<sup>[20]</sup>. QS participates in various social behaviors of bacteria, including *Lactobacillus*, such as biofilm formation and adhesion<sup>[20]</sup>. Therefore, the expression level of *luxS* can influence the biofilm formation and adhesion abilities of the LR-1 strain. The *rpoN* gene encodes the  $\sigma_{54}$  factor, which is involved in

various physiological processes, including carbon source metabolism, detoxification system control, and extracellular alginate production<sup>[21]</sup>. In *Vibrio fischeri*, the  $\sigma 54$  factor regulates the expression of the *syp* gene cluster, which is associated with polysaccharide production, biofilm formation, and adhesion<sup>[22]</sup>. Additionally,  $\sigma 54$  has also been found to regulate biofilm formation and adhesion in *Bacillus cereus*, *Enterococcus faecalis*, and *Escherichia coli* K12<sup>[23-25]</sup>. In conclusion, *tuf*, *luxS* and *rpoN* are all multifunctional moonlighting genes that have been associated with biofilm formation and other critical physiological behaviors in various strains. Moreover, our previous research has confirmed that they are key genes regulating biofilm formation and other phenotypes in *Lactobacillus*. In this study, the overexpression of the *rbk* gene significantly enhanced their expression levels. These results suggest that the *rbk* gene may positively regulate biofilm formation and adhesion abilities of the LR-1 strain by upregulating the expression of these key moonlighting genes. However, the hierarchical relationships between the *rbk* gene and these genes, both upstream and downstream, are not clearly established and require further research for in-depth analysis.

#### 2.4 The effect of *rbk* overexpression on the metabolic profile of the LR-1 strain

This study employed PCA, PLS-DA, and OPLS-DA to conduct multivariate statistical analysis on the metabolites of *rbk*-pMG76e-LR-1 and pMG76e-LR-1, with the results shown in Figure 4A–4C. PCA is a straightforward non-parametric technique that projects complex metabolic data into a lower-dimensional space, allowing for the

identification of potential relationships and uncovering intricate internal data structures<sup>[26]</sup>. As illustrated in Figure 4A, the PCA results revealed a distinct variation between the two groups. The sum of the components (1 and 2) accounted for 71.60% of the total variance in the positive mode and 74.40% in the negative mode, respectively. PLS-DA is a well-established linear classification method that is effective for analyzing complex metabolic data sets<sup>[27]</sup>. In the positive mode, the  $R^2(X)$ ,  $R^2(Y)$ , and  $Q^2$  values were 0.71, 0.99, 0.99, respectively, while in the negative mode, they were 0.74, 0.99, and 0.99 (Figure 4B). In contrast to PCA and PLS-DA, OPLS-DA can differentiate between predictive and non-predictive (orthogonal) changes<sup>[28]</sup>. The  $R^2(X)$ ,  $R^2(Y)$ , and  $Q^2$  values of the OPLS-DA model were 0.71, 0.99, and 0.98 in the positive mode, and 0.74, 0.99, and 0.99 in the negative mode, as shown in Figure 4C. All three methods can be used for integrative analysis of metabolomic profiles of *Lactobacillus* samples. Lee and colleagues applied PCA and PLS-DA to analyze samples of *Lactobacillus sakei* at different growth stages based on their metabolites<sup>[29]</sup>. Similarly, Tomita and others employed PCA and OPLS-DA to clearly distinguish the metabolic profile of vegetable juice samples fermented by various *Lactobacillus* strains<sup>[30]</sup>. In this study, based on the differential metabolite data, all three analytical methods were able to distinguish between *rbk*-pMG76e-LR-1 and pMG76e-LR-1 samples, indicating that *rbk* overexpression significantly affected the metabolic profile LR-1.

The differential metabolites of the *rbk*-pMG76e-LR-1 and pMG76e-LR-1 samples are shown in Figure 5A–5B for positive and negative

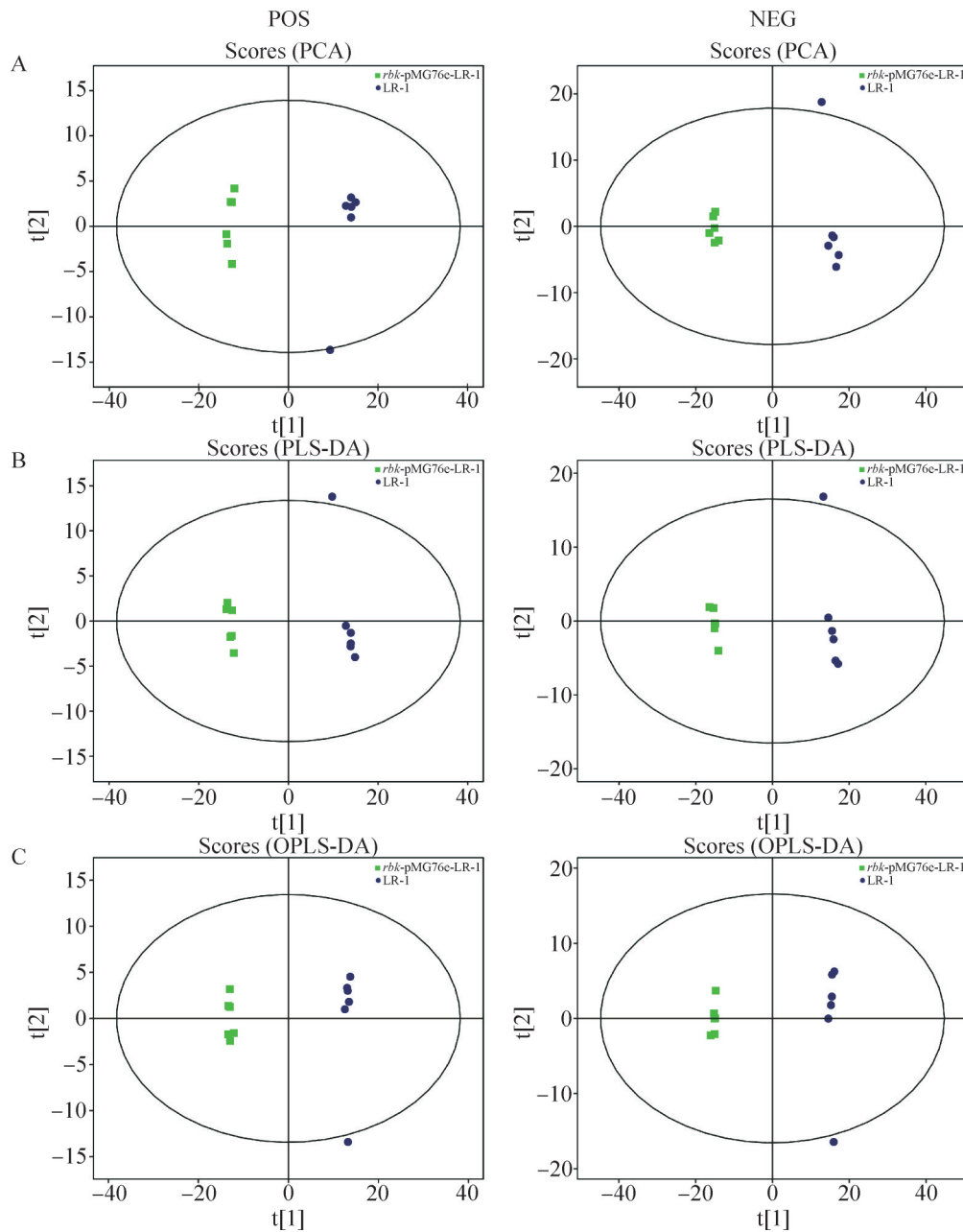


Figure 4 The PCA (A), PLS-DA (B) and OPLS-DA (C) analysis of the metabolites from *rbk*-pMG76e-LR-1 and pMG76e-LR-1. POS: Positive ion model; NEG: Negative ion model.

ion modes, respectively. In the positive ion mode, a total of 83 differential metabolites were detected, while in the negative ion mode, 78 differential metabolites were identified. Some substance fragments were detected in both ion modes, resulting in a total of 145 unique differential

metabolites across both groups. Among them, the top five significantly upregulated differential metabolites due to *rbk* gene introduction were D-ribulose-5-phosphate (49.99 folds), L-rhamnose (28.66 folds), N-acetyl-D-lactosamine (26.19 folds), glutathione (GSH) (16.42 folds), and UDP-N-

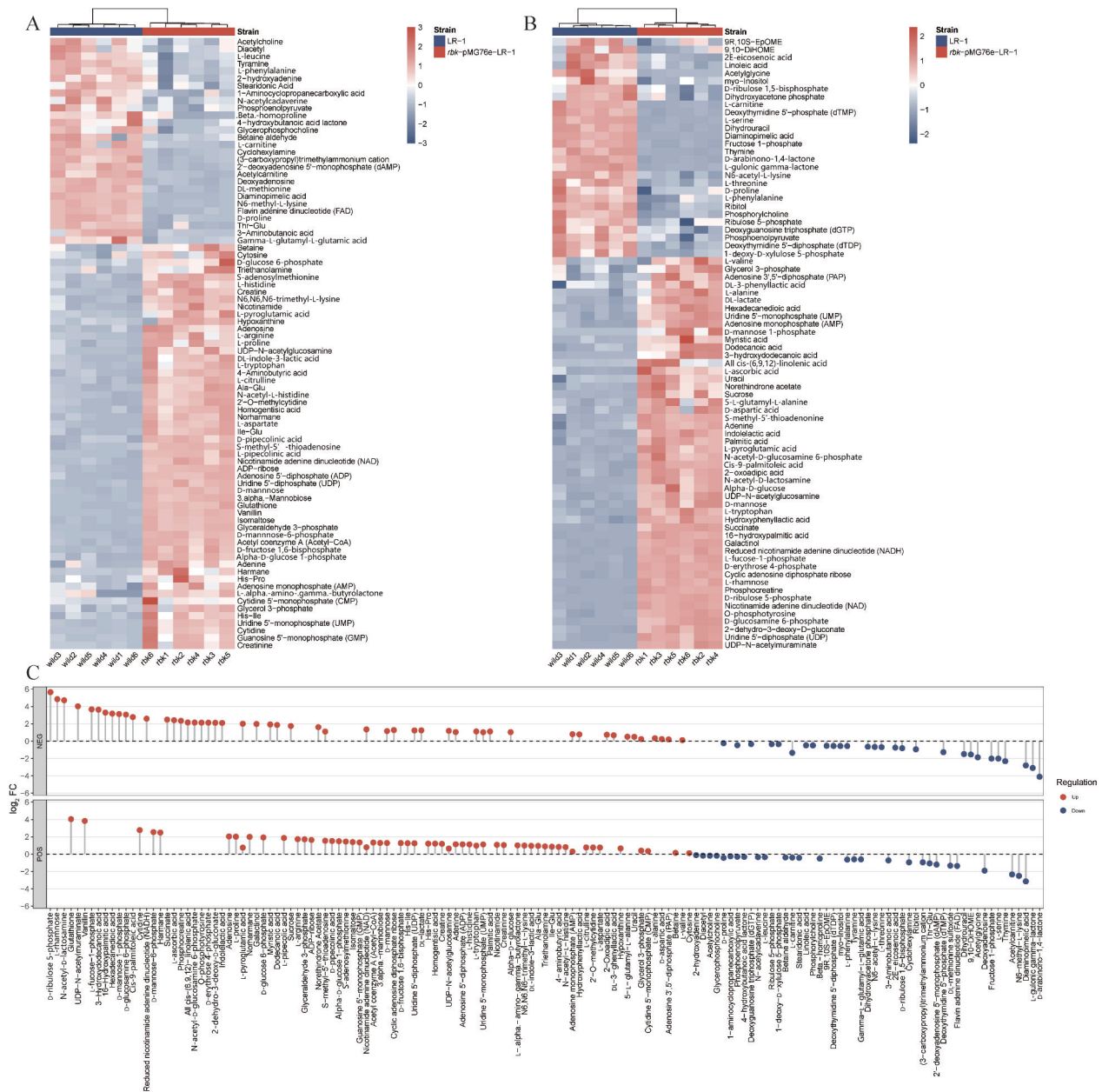


Figure 5 The differential metabolites of the *rbk*-pMG76e-LR-1 and pMG76e-LR-1 samples. The heatmap analysis of significantly differential metabolites in *rbk*-pMG76e-LR-1 and pMG76e-LR-1 in the positive ion model (A) and in the negative ion model (B). The fold changes of the differential metabolites in *rbk*-pMG76e-LR-1 compared to pMG76e-LR-1 (C). POS: Positive ion model; NEG: Negative ion model.

acetylmuraminate (16.21 folds). Conversely, the top five significantly downregulated differential metabolites were D-arabinono-1,4-lactone (0.06 folds), diaminopimelic acid (0.11 folds), L-gulonic- $\gamma$ -lactone (0.12 folds),

$N_6$ -methyl-L-lysine (0.18 folds), and acetyl carnitine (0.20 folds) (Figure 5C).

This study further predicted the correlation between differential metabolites and phenotypes,

with results shown in Figure 6. The predictive analysis indicates that a total of 112 differential metabolites exhibited strong correlations with the phenotypes assessed in this study ( $P < 0.01$ , absolute value of the coefficient index  $> 0.9$ ), with 77 being positively correlated and 35 negatively correlated. Among these, the phenotype of biofilm formation was positively correlated with 42 differential metabolites and negatively correlated with 27 metabolites. The adhesion phenotype was positively correlated with 6 differential metabolites and negatively with 1 metabolite. The impact of *rbk* gene introduction on metabolites will be further analyzed and discussed in the following sections

from a metabolic pathway perspective.

### 2.4.1 Central carbon metabolism changes

Among the 145 differential metabolites, 18 substances (12.41%) belong to the central carbon metabolism pathway, as shown in Figure 7. The analysis indicates that the introduction of the *rbk* gene leads to the downregulation of three substances: D-xylulose-5P, glycerone-P, and phosphoenolpyruvate, which were reduced to 0.79, 0.88 and 0.81 folds, respectively, while the remaining 15 substances were all upregulated. These differential metabolites are distributed across four carbon metabolic pathway: the Embden-Meyerhof-Parnas (EMP) pathway, the Entner-Doudoroff (ED) pathway, the

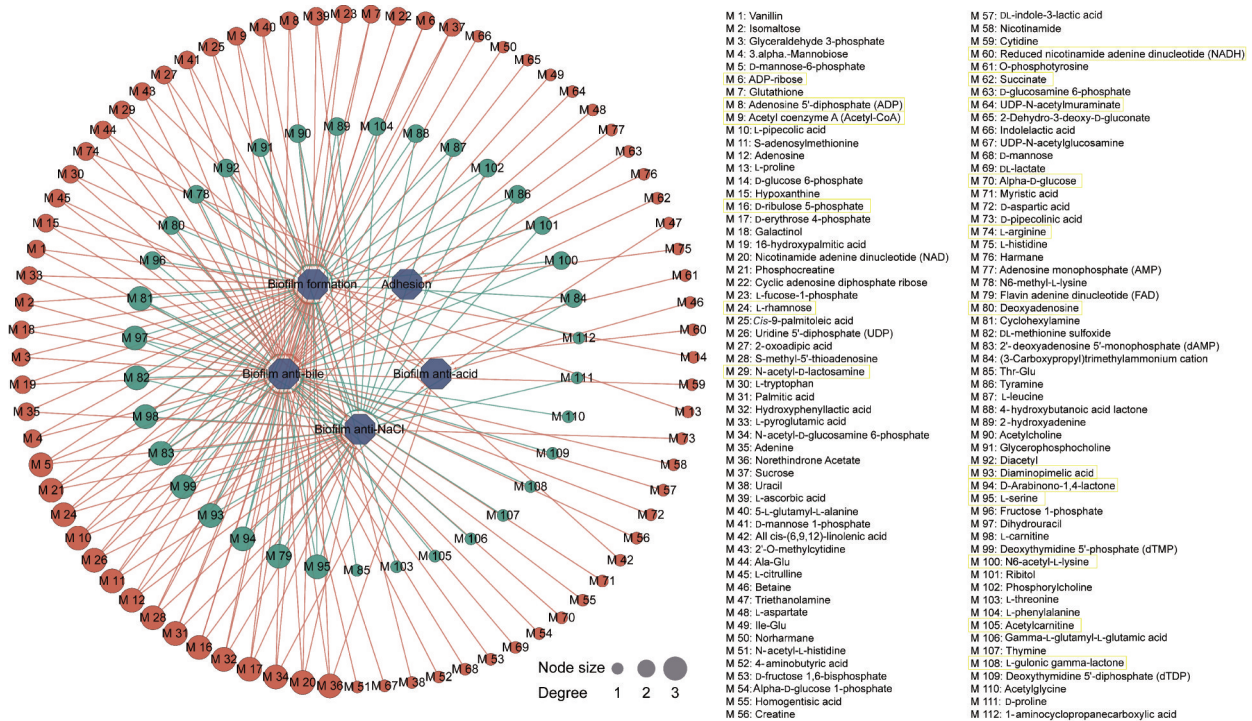


Figure 6 The Pearson correlation network diagram between differential metabolites and biofilm formation as well as adhesion is presented. The absolute value of correlation coefficient  $> 0.9$ ,  $P < 0.01$ . Red circles represent differential metabolites that have a positive correlation with biofilm formation and adhesion, while green circles represent differential metabolites that are negatively correlated with these phenotypes. Blue circles indicate the phenotypes of biofilm formation and adhesion capacity. The larger the circle, the more associated substances it contains. Red lines indicate positive correlations, while green lines indicate negative correlations.

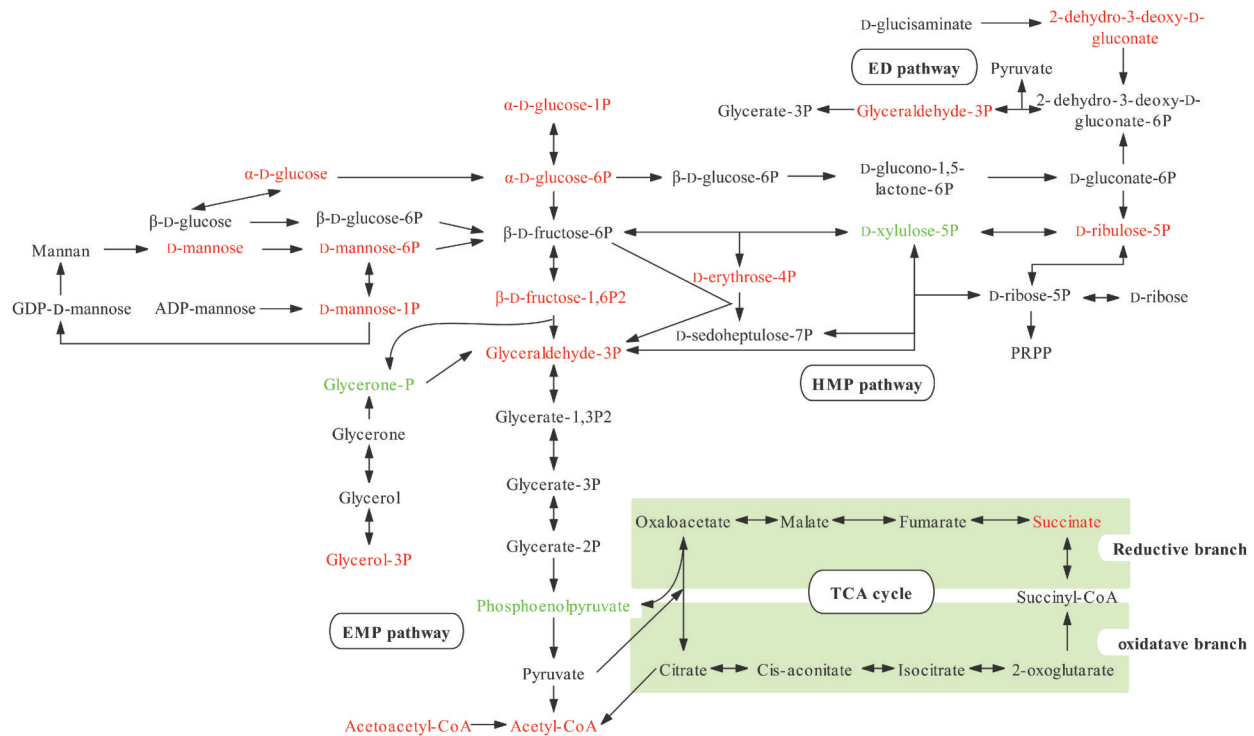


Figure 7 Changes in metabolites in the central carbon metabolism pathway following *rbk* gene introduction are highlighted. Metabolites with increased abundance are marked in red, while those with decreased abundance are marked in green. P: Phosphate; PRPP: 5-phospho-alpha-D-ribose 1-diphosphate.

hexose monophosphate (HMP) pathway, and the tricarboxylic acid (TCA) cycle<sup>[31-33]</sup>.

In the EMP pathway, the introduction of the *rbk* gene results in the upregulation of  $\alpha$ -D-glucose (2.05 folds),  $\alpha$ -D-glucose-6P (3.80 folds),  $\beta$ -D-fructose-1,6P2 (2.43 folds), and glyceraldehyde-3P (3.28 folds). Additionally, these four substances are located upstream of the EMP pathway<sup>[32]</sup>, suggesting that *rbk* overexpression may enhance the strain LR-1's ability to utilize the EMP pathway to convert glucose into glyceraldehyde-3P. In the ED pathway, 2-dehydro-3-deoxy-D-gluconate (4.33 folds) and glyceraldehyde-3P (3.28 folds) were found to be upregulated. Microorganism can convert glucose into pyruvate *via* the ED pathway in just four steps<sup>[33]</sup>. These results indicate that *rbk* overexpressing

strains can utilize the ED pathway, rather than the EMP pathway to convert glyceraldehyde-3P into pyruvate. Previous studies have shown that *Campylobacter coli* B13117 can enhance its environmental tolerance by altering its metabolism to utilize the ED pathway more extensively for the conversion of glucose into glucose-6P and fructose-6P<sup>[33]</sup>. Furthermore, in the EMP pathway, the levels of D-mannose and D-glucose were upregulated in the *rbk* overexpressing strains. These two monomers are important precursor substances for the synthesis of extracellular polysaccharides. Their upregulation may accelerate the efficiency of extracellular polysaccharide synthesis (EPS), which is crucial for biofilm formation and adhesion capacity<sup>[34-36]</sup>.

In the HMP pathway, *rbk* overexpression led

to a significant upregulation of D-ribulose-5P (49.99 folds), the most prominently upregulated metabolite among all the substances<sup>[32]</sup>. The *rbk* gene is responsible for converting D-ribose to D-ribose-5P, which can then be transformed into D-ribulose-5P<sup>[8,37]</sup>. Our results indicate that *rbk* overexpression enhances the strain LR-1's ability to convert  $\alpha$ -D-glucose-6P into D-ribulose-5P via the HMP pathway. Studies have shown that *Lactiplantibacillus* can enhance its environmental tolerance by altering its metabolic pathways<sup>[38]</sup>. In this study, the overexpression of the *rbk* gene affects the central carbon metabolism pathway of LR-1, which may play a role in the alteration of the strain's biofilm formation and adhesion capacity.

### 2.4.2 Amino acid metabolism changes

In the context of the 145 differential metabolites induced by *rbk* overexpression, 15 of

these metabolites (10.34%) were identified to be located in the amino acid metabolism pathway, as shown in Figure 8. Among them, four amino acids were downregulated: phenylalanine decreased to 0.65 folds, L-leucine decreased to 0.79 folds, serine decreased to 0.25 folds, and threonine decreased to 0.62 folds. Conversely, 11 amino acids were upregulated: L-alanine increased to 1.26 folds, L-aspartate increased to 1.70 folds, L-histidine increased to 2.18 folds, S-adenosyl-L-methionine increased to 2.74 folds, proline increased to 4.04 folds, arginine increased to 3.31 folds, L-valine increased to 1.08 folds, tryptophan increased to 1.98 folds, S-adenosyl-4-aminobutanoate increased to 1.78 folds, acetyl-CoA increased to 2.53 folds, and succinate increased to 5.59 folds.

The results indicate that the majority of amino acid levels increased in the *rbk*-pMG76e-LR-1

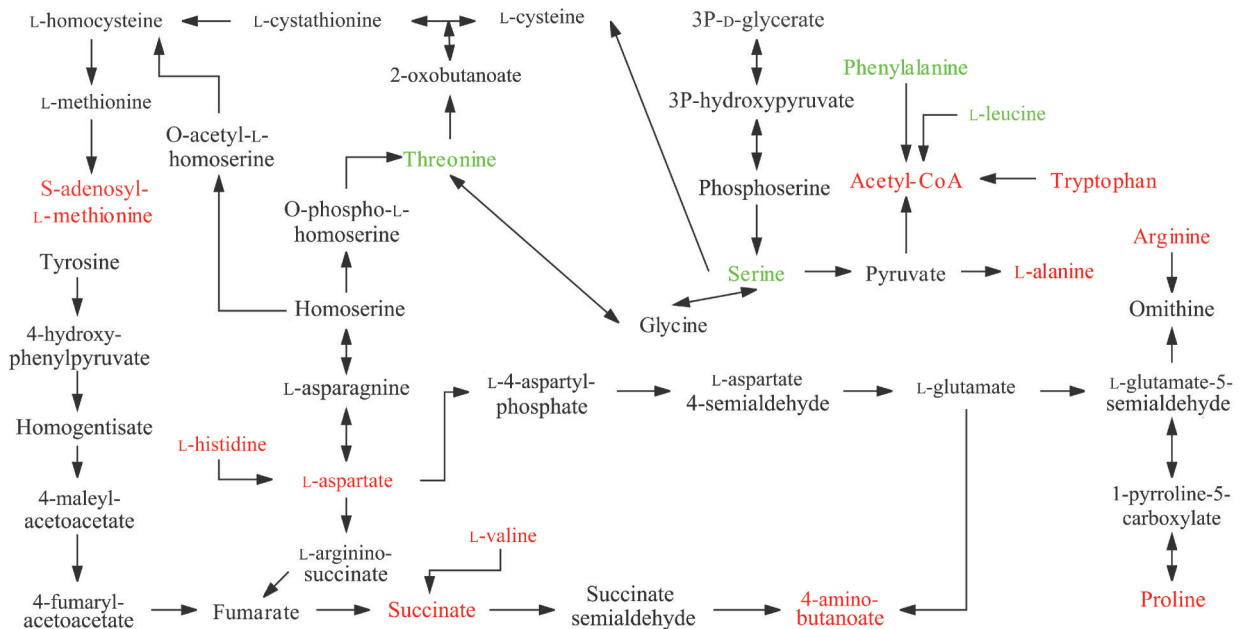


Figure 8 Changes in metabolites in the amino acid metabolism pathway following *rbk* gene introduction are highlighted. Metabolites with increased abundance are marked in red, while those with decreased abundance are marked in green. P: Phosphate.

recombinant strain, suggesting that the overexpression of the *rbk* gene enhances amino acid metabolism. Given that amino acids are important biochemical precursors, the increased activity of amino acid metabolism may lead to significant changes in physiological phenotypes. For instance, previous studies have shown that *L. plantarum* can resist acid stress by upregulating the abundance of aspartate and arginine<sup>[39]</sup>. In this study, both of these amino acids were significantly upregulated, which may explain why the *rbk* overexpressing strain exhibits a stronger biofilm formation in acidic conditions. Furthermore, other studies have found that arginine and proline significantly influence the adhesion ability of *L. plantarum* ATCC 14917<sup>[40]</sup>. The upregulation of these two amino acids in this study may be related to the enhanced adhesion capacity of the *rbk* overexpressing strain. However, the specific relationships among them still require further investigation.

### 2.4.3 Energy metabolism changes

Figure 9 shows that out of the 145 different metabolites, 14 (9.66%) are associated with the energy metabolism pathway. In the *rbk* overexpressing strain, the levels of NADH, NAD<sup>+</sup>, succinate, and ADP increased to 6.02, 2.55, 5.59 and 2.19 folds, respectively, during oxidative phosphorylation. During methane metabolism, D-ribulose-5P increased dramatically (49.99 folds), while D-glyceraldehyde-3P (3.28 folds), D-fructose-1,6P2 (2.43 folds), and acetyl-CoA (2.53 folds) also showed significant increases. However, glycero-P (0.88 folds), L-serine (0.25 folds), and phosphoenolpyruvate (0.81 folds) decreased in the *rbk*-pMG76e-LR-1 strain. In the context of sulfur metabolism, only L-serine, PAP, and succinate

were detected, with values of 0.25, 1.15 and 5.59 folds, respectively.

The total NAD(H) plays a crucial role in whole-cell biochemical redox transformations<sup>[37]</sup>. The *rbk*-pMG76e-LR-1 strain exhibited increases in both NAD(H) and its related products, including succinate and acetyl-CoA. Succinate participates in the conversion of fumarate to succinate, generating NAD<sup>+</sup>, while acetyl-CoA is involved in the conversion of pyruvate to acetyl-CoA, producing NADH. This suggests that the elevated levels of NAD(H) may stimulate related biochemical redox reactions, leading to the production of additional reaction products. Furthermore, *rbk*-pMG76e-LR-1 exhibited higher ADP content. The release of energy from ATP by breaking phosphate bonds, while simultaneously producing ADP, indicates that *rbk* overexpression results in enhanced energy metabolism and increased energy production.

These results suggest that energy metabolism is likely more active in the *rbk*-pMG76e-LR-1 strain. The biofilm formation process is known to be energy-consuming, as the synthesis of the biofilm matrix requires significant metabolic resources<sup>[41]</sup>. Therefore, the increased energy metabolism observed in *rbk*-pMG76e-LR-1 may enhance biofilm formation and improve environmental tolerance. Additionally, studies have shown that *L. plantarum* FS5-5 can withstand salt stress by boosting energy metabolism<sup>[42]</sup>.

### 2.4.4 Nucleotide metabolism changes

Figure 10 illustrates that out of the 145 different metabolites, 21 (14.48%) are linked to the nucleotide metabolism pathway. In this study, most metabolites associated with nucleotide metabolism exhibited higher abundance in the *rbk*-pMG76e-LR-1 strain.

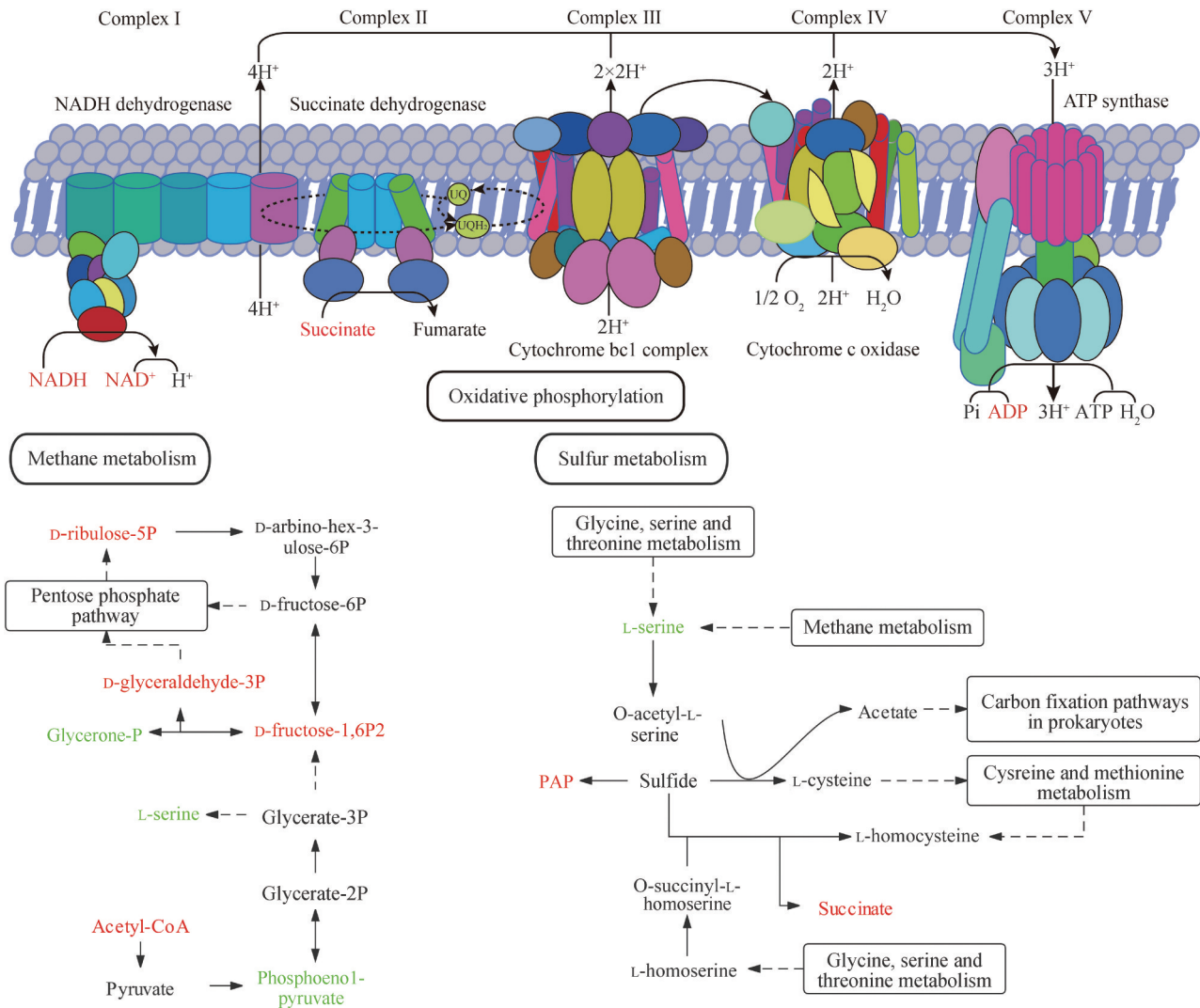


Figure 9 Changes in metabolites in the energy metabolism pathway following *rbk* gene introduction are highlighted. Metabolites with increased abundance are marked in red, while those with decreased abundance are marked in green. P: Phosphate; PAP: Adenosine 3',5'-diphosphate.

During purine metabolism, several metabolites increased significantly, including ADP-ribose (3.12 folds), GMP (2.56 folds), hypoxanthine (1.59 folds), AMP (1.23 folds), adenosine (4.13 folds), adenine (2.30 folds), and ADP (2.19 folds). In contrast, levels of FAD (0.39 folds), dGTP (0.79 folds), dAMP (0.44 folds), and deoxyadenosine (0.27 folds) decreased in *rbk*-pMG76e-LR-1. Previous research has indicated that the synthesis of purine nucleotide

is positively correlated with biofilm formation<sup>[9,42]</sup>. Therefore, it can be hypothesized that the increase in purine metabolites may contribute to enhanced biofilm formation in the *rbk*-pMG76e-LR-1 strain.

In terms of pyrimidine metabolism, metabolites such as uracil, UMP, cytosine, UDP, cytidine, and CMP increased to 1.41, 2.17, 1.08, 2.39, 6.83 and 1.27 folds, respectively, in the *rbk*-pMG76e-LR-1 recombinant strain. However, dihydrouracil, thymine,

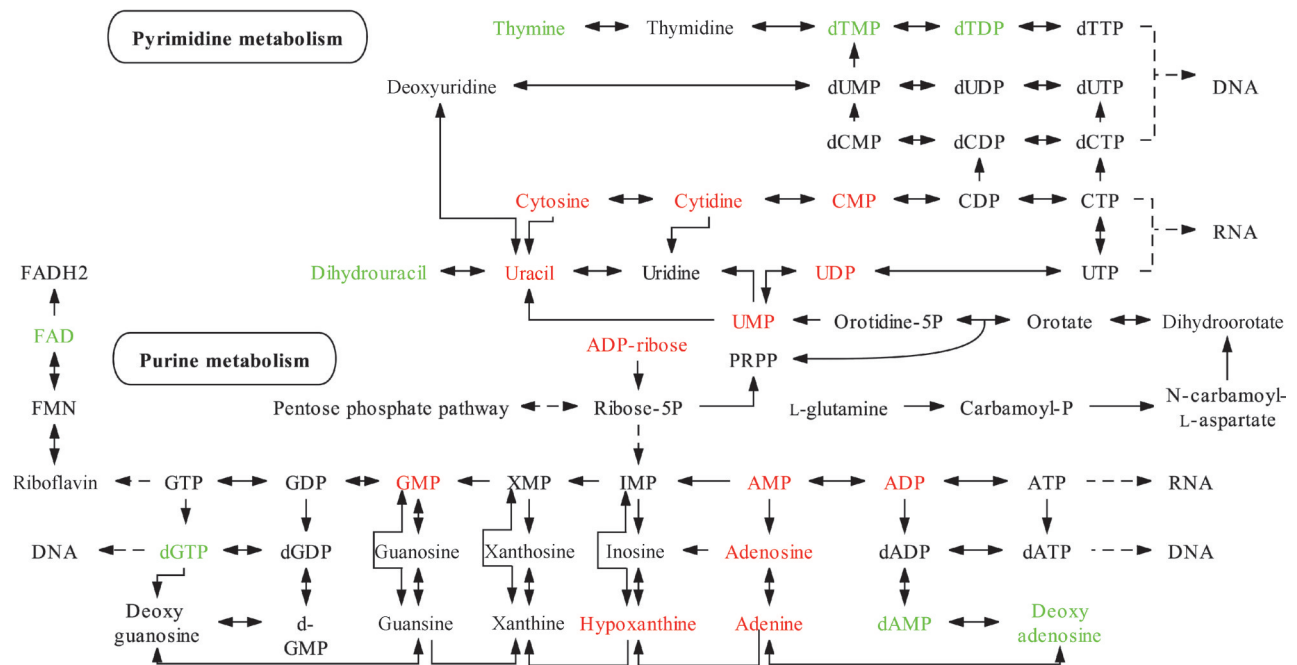


Figure 10 Changes in metabolites in the nucleotide metabolism pathway following *rbk* gene introduction are highlighted. Metabolites with increased abundance are marked in red, while those with decreased abundance are marked in green.

dTMP, and dTDP showed decreases of 0.36, 0.20, 0.41 and 0.68 folds, respectively. Notably, uracil has been reported to influence all three known QS pathways in *Pseudomonas aeruginosa*, and mutations related to uracil can disrupt biofilm formation by this strain<sup>[41]</sup>. Thus, it is speculated that the increased level of uracil may promote biofilm development in *rbk*-pMG76e-LR-1.

#### 2.4.5 Changes in other metabolites

Some metabolites were not clearly categorized within the previously mentioned pathways but are closely linked to biofilm formation and stress resistance. For instance, L-rhamnose increased to 28.66 folds in the *rbk*-pMG76e-LR-1 recombinant strain. This metabolite is considered crucial for the growth of *Streptococcus mutans*, and disruption in its biosynthesis can heighten the strain's susceptibility

to acid and oxidative stress<sup>[43]</sup>. Additionally, other studies have indicated that L-rhamnose biosynthesis can positively stimulate biofilm formation in *Listeria monocytogenes* and *Flavobacterium columnare*<sup>[44-45]</sup>. Therefore, it is hypothesized that the increased L-rhamnose levels in *rbk*-pMG76e-LR-1 promote both biofilm formation and stress resistance.

Moreover, several substances with potential health benefits were found to be elevated in the overexpressed *rbk* strain. Levels of  $\gamma$ -amino butyric acid (GABA), glutathione (GSH), and S-adenosyl methionine (SAM) increased to 1.78, 16.42 and 2.74 folds, respectively, in *rbk*-pMG76e-LR-1. GSH and SAM are recognized for their liver-protective properties, helping to prevent and treat various liver injuries and diseases<sup>[46]</sup>. Additionally, GABA

plays a vital role in the resistance of LAB to acidic and bile salt environments<sup>[47-48]</sup>. The increases in these metabolites suggest that the overexpressed *rbk* strain enhances stress resistance and holds potential for improved health benefits.

### 2.5 Metabolites enhance the biofilm formation and adhesion ability of LR-1 strain

The influence of 8 metabolites on the biofilm formation ability of LR-1 strain is shown in Figure 11A. The biofilm formation ability of LR-1 strain treated with metabolites was slightly improved. L-proline, rhamnose and NADH significantly enhanced the biofilm formation ability of LR-1. L-proline increased by 1.27 folds, rhamnose increased by 1.39 folds, and NADH increased by 1.25 folds. However, other metabolites had no significant impact on its biofilm formation.

The LR-1 strains treated by two treatment methods were used for adhesion to HT-29 cells,

and the results are shown in Figure 11B. Compared with the control group, various metabolites all increased the adhesion ability of LR-1 to a certain extent, and the adhesion rate of bacteria in the met-LR-1-HT-29 group to HT-29 cells was higher than that of bacteria in the met-LR-1-post-LR-1 group. In the adhesion test of the met-LR-1-post-LR-1 group, D-mannose-6-phosphate significantly increased the adhesion ability of LR-1 (by about 1.30 folds), and other metabolites had no significant impact on the adhesion ability of LR-1. However, in the adhesion test of the met-LR-1-HT-29 group, L-proline, L-arginine, rhamnose, N-acetyl-D-lactosamine, D-mannose-6-phosphate, and NADH significantly increased the adhesion ability of LR-1. Proline increased by 1.40 folds, arginine increased by 1.33 folds, rhamnose increased by 1.41 folds, N-acetyl-D-lactosamine increased by 1.38 folds, D-mannose-6-phosphate increased by 1.44 folds, and NADH increased by 1.52 folds.

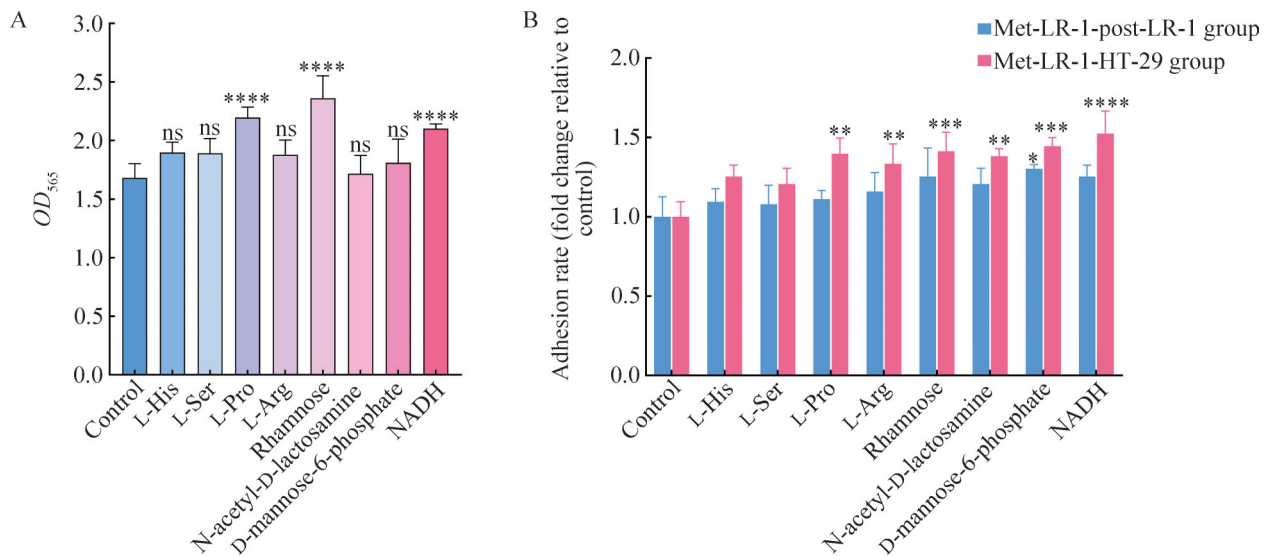


Figure 11 Effect of exogenously added metabolites on biofilm formation (A) and adhesion ability (B) of LR-1 strain. The data obtained from three separate experiments are presented as mean±SD. \*\*\*\*:  $P < 0.0001$ ; \*\*\*:  $P < 0.001$ ; \*\*:  $P < 0.01$ ; \*:  $P < 0.05$ ; ns: No significant.

The results showed that proline and arginine could significantly enhance the adhesion ability of LR-1, which was consistent with the finding of Wan et al. that arginine and proline would significantly affect the adhesion ability of *Lactobacillus plantarum* ATCC 14917<sup>[40]</sup>. And the adhesiveness of bacteria is an important factor in biofilm formation. As the adhesion ability of bacteria increases, their ability to form biofilms also increases. Some studies have shown that amino acids can participate in the metabolic pathways of lactic acid bacteria, promote the synthesis of adhesion-related substances (such as extracellular polysaccharide EPS and S-layer protein), thereby improving the adhesion ability of lactic acid bacteria<sup>[49]</sup>, and regulate the quorum-sensing system of lactic acid bacteria through signal transduction pathways, thereby affecting the adhesion behavior of lactic acid bacteria<sup>[50]</sup>. Rhamnose, N-acetyl-D-lactosamine, and D-mannose-6-phosphate, as products in the carbon metabolism process, are important precursor substances for the synthesis of EPS. Exogenous addition may accelerate the synthesis efficiency of EPS, thereby affecting biofilm formation and adhesion ability. NADH is a key reductant in energy metabolism. By participating in processes such as glycolysis and oxidative phosphorylation, it provides energy for biofilm formation and maintenance<sup>[51]</sup>. A high-level NADH/NAD<sup>+</sup> ratio may create a more suitable intracellular environment for biofilm formation. Under such conditions, cells may be more inclined to express genes related to biofilm formation, such as genes encoding cell-surface proteins and polysaccharide synthases<sup>[52]</sup>. These increased gene expressions may enhance the adhesion ability of lactic acid

bacteria. These results may explain the reasons for the significant up-regulation of arginine, proline, rhamnose, N-acetyl-D-lactosamine, D-mannose-6-phosphate, and NADH contents and the improvement of biofilm formation and adhesion ability after the over-expression of the *rbk* gene in this study.

### 3 Conclusion

This study demonstrates that the overexpression of the *rbk* gene enhances the biofilm formation and adhesion capabilities of *L. paraplantarum* LR-1 while also upregulating the transcriptional levels of the *tuf*, *luxS*, and *rpoN* genes. Additionally, untargeted metabolomic analysis reveals that this overexpression leads to significant changes in 145 metabolites of *L. paraplantarum* LR-1, with 112 of these metabolites showing a strong correlation with biofilm formation and adhesion. Furthermore, the abundance of most metabolites related to central carbon, amino acid, energy, and nucleotide metabolism is higher in the *rbk*-pMG76e-LR-1 strain. These findings suggest that the overexpression of the *rbk* gene enhances the activity of these metabolic pathways. In addition, it was verified by exogenous addition of metabolites that some of the metabolites could significantly increase the biofilm formation and adhesion ability of LR-1 strain, which also indicates on the side that the overexpression of the *rbk* gene would have an effect on its biofilm formation and adhesion ability. Overall, this study indicates that the *rbk* gene plays a crucial role in metabolic regulation, significantly promoting the biofilm formation and adhesion abilities of *Lactobacillus* strains.

## References

- [1] SUEZ J, ZMORA N, SEGAL E, ELINAV E. The pros, cons, and many unknowns of probiotics[J]. *Nature Medicine*, 2019, 25(5): 716-729.
- [2] KHORUTS A, HOFFMANN DE, BRITTON RA. Probiotics: promise, evidence, and hope[J]. *Gastroenterology*, 2020, 159(2): 409-413.
- [3] JANDL B, DIGHE S, BAUMGARTNER M, MAKRIATHIS A, GASCHÉ C, MUTTENTHALER M. Gastrointestinal biofilms: endoscopic detection, disease relevance, and therapeutic strategies[J]. *Gastroenterology*, 2024, 167(6): 1098-1112.e5.
- [4] LI ZH, BEHRENS AM, GINAT N, TZENG SY, LU XG, SIVAN S, LANGER R, JAKLENEC A. Biofilm-inspired encapsulation of probiotics for the treatment of complex infections[J]. *Advanced Materials*, 2018, 30(51): e1803925.
- [5] LI SY, SUN HX, LI JH, ZHAO YJ, WANG RY, XU L, DUAN CY, LI JL, WANG Z, LIU QM, WANG Y, OUYANG SY, SHEN XH, ZHANG L. Autoinducer-2 and bile salts induce c-di-GMP synthesis to repress the T3SS *via* a T3SS chaperone[J]. *Nature Communications*, 2022, 13(1): 6684.
- [6] LIU L, WU RY, ZHANG JL, SHANG N, LI PL. D-Ribose interferes with quorum sensing to inhibit biofilm formation of *Lactobacillus paraplantarum* L-ZS9[J]. *Frontiers in Microbiology*, 2017, 8: 1860.
- [7] POKUSAIEVA K, NEVES AR, ZOMER A, O'CONNELL-MOTHERWAY M, MacSHARRY J, CURLEY P, FITZGERALD GF, van SINDEREN D. Ribose utilization by the human commensal *Bifidobacterium breve* UCC2003[J]. *Microbial Biotechnology*, 2010, 3(3): 311-323.
- [8] KORI LD, HOFMANN A, PATEL BKC. Expression, purification, crystallization and preliminary X-ray diffraction analysis of a ribokinase from the thermohalophile *Halothermothrix orenii*[J]. *Acta Crystallographica Section F, Structural Biology and Crystallization Communications*, 2012, 68(Pt 2): 240-243.
- [9] MARTINEZ S, GARCIA JG, WILLIAMS R, ELMASSRY M, WEST A, HAMOOD A, HURTADO D, GUDENKAUF B, VENTOLINI G, SCHLABRITZ-LOUTSEVITCH N. *Lactobacilli* spp.: real-time evaluation of biofilm growth[J]. *BMC Microbiology*, 2020, 20(1): 64.
- [10] CABRAL MP, SOARES NC, ARANDA J, PARREIRA JR, RUMBO C, POZA M, VALLE J, CALAMIA V, LASA I, BOU G. Proteomic and functional analyses reveal a unique lifestyle for *Acinetobacter baumannii* biofilms and a key role for histidine metabolism[J]. *Journal of Proteome Research*, 2011, 10(8): 3399-3417.
- [11] LIU L, CHEN X, ZHANG CY, DENG J, XIAO H, RAO Y. *Lactiplantibacillus* biofilm and planktonic cells ameliorate ulcerative colitis in mice *via* immunoregulatory activity, gut metabolism and microbiota modulation[J]. *Food & Function*, 2023, 14(20): 9181-9193.
- [12] LIVAK KJ, SCHMITTGEN TD. Analysis of relative gene expression data using real-time quantitative PCR and the 2<sup>-ΔΔC<sub>T</sub></sup> Method[J]. *Methods*, 2001, 25(4): 402-408.
- [13] 陈星, 郭书玉, 陶雨飞, 邓西, 杨淑慧, 涂明霞, 吴艾玲, 马偲臆, 饶瑜, 刘蕾. 糖酵解途径相关基因与植物乳杆菌生理行为的相关性[J]. *食品科学*, 2021, 42(22): 113-124.
- CHEN X, GUO SY, TAO YF, DENG X, YANG SH, TU MX, WU AL, MA SY, RAO Y, LIU L. Association of the expression of glycolytic pathway-related genes with the physiological behavior of *Lactobacillus plantarum*[J]. *Food Science*, 2021, 42(22): 113-124 (in Chinese).
- [14] CHO YJ, SONG HY, BEN AMARA H, CHOI BK, EUNJU R, CHO YA, SEOL Y, LEE Y, KU Y, RHYU IC, KOO KT. *In vivo* inhibition of *Porphyromonas gingivalis* growth and prevention of periodontitis with quorum-sensing inhibitors[J]. *Journal of Periodontology*, 2016, 87(9): 1075-1082.
- [15] LIU L, DENG J, GUO SY, LI YF, WANG LY, LIU YY, XV P, RAO Y. Stress tolerance and characterization of biofilm-like probiotic bacteria encapsulated in calcium pectin beads[J]. *LWT*, 2023, 184: 115072.
- [16] RIEU A, AOUDIA N, JEGO G, CHLUBA J, YOUSFI N, BRIANDET R, DESCHAMPS J, GASQUET B, MONEDERO V, GARRIDO C, GUZZO J. The biofilm mode of life boosts the anti-inflammatory properties of *Lactobacillus*[J]. *Cellular Microbiology*, 2014, 16(12): 1836-1853.
- [17] CALDAS TD, EL YAAGOUBI A, RICCHARME G. Chaperone properties of bacterial elongation factor EF-tu[J]. *Journal of Biological Chemistry*, 1998, 273(19): 11478-11482.
- [18] DHANANI AS, BAGCHI T. The expression of adhesin EF-Tu in response to mucin and its role in *Lactobacillus* adhesion and competitive inhibition of enteropathogens to mucin[J]. *Journal of Applied Microbiology*, 2013, 115(2): 546-554.
- [19] RAMIAH K, van REENEN CA, DICKS LMT. Expression of the mucus adhesion gene *mub*, surface layer protein *slp* and adhesion-like factor EF-TU of *Lactobacillus acidophilus* ATCC 4356 under digestive stress conditions, as monitored with real-time PCR[J]. *Probiotics and Antimicrobial Proteins*, 2009, 1(1): 91.
- [20] LIU L, WU RY, ZHANG JL, LI PL. Overexpression of *luxS* promotes stress resistance and biofilm formation of *Lactobacillus paraplantarum* L-ZS9 by regulating the expression of multiple genes[J]. *Frontiers in Microbiology*, 2018, 9: 2628.
- [21] MAXSON ME, DARWIN AJ. Multiple promoters control expression of the *Yersinia enterocolitica* phage-shock-protein A (*pspA*) operon[J]. *Microbiology*, 2006, 152(Pt 4): 1001-1010.
- [22] YIP ES, GRUBLESKY BT, HUSSA EA, VISICK KL. A novel, conserved cluster of genes promotes symbiotic colonization and sigma-dependent biofilm formation by

- Vibrio fischeri*[J]. *Molecular Microbiology*, 2005, 57(5): 1485-1498.
- [23] BELIK AS, TARASOVA NN, KHMEL' IA. Regulation of biofilm formation in *Escherichia coli* K12: effect of mutations in HNS StpA, lon, and rpoN genes[J]. *Molekuliarnaia Genetika, Mikrobiologiya I Virusologiya*, 2008(4): 3-5.
- [24] HAYRAPETYAN H, TEMPELAARS M, NIEROP GROOT M, ABEE T. *Bacillus cereus* ATCC 14579 RpoN (sigma 54) is a pleiotropic regulator of growth, carbohydrate metabolism, motility, biofilm formation and toxin production[J]. *PLoS One*, 2015, 10(8): e0134872.
- [25] IYER VS, HANCOCK LE. Deletion of  $\sigma(54)$  (rpoN) alters the rate of autolysis and biofilm formation in *Enterococcus faecalis*[J]. *Journal of Bacteriology*, 2012, 194(2): 368-375.
- [26] NYAMUNDANDA G, BRENNAN L, GORMLEY IC. Probabilistic principal component analysis for metabolomic data[J]. *BMC Bioinformatics*, 2010, 11: 571.
- [27] SINDT NM, ROBISON F, BRICK MA, SCHWARTZ HF, HEUBERGER AL, PRENNI JE. MALDI-TOF-MS with PLS modeling enables strain typing of the bacterial plant pathogen *Xanthomonas axonopodis*[J]. *Journal of the American Society for Mass Spectrometry*, 2018, 29(2): 413-421.
- [28] BYLESJÖ M, RANTALAINEN M, CLOAREC O, NICHOLSON JK, HOLMES E, TRYGG J. OPLS discriminant analysis: combining the strengths of PLS-DA and SIMCA classification[J]. *Journal of Chemometrics*, 2006, 20(8/9/10): 341-351.
- [29] LEE SB, RHEE YK, GU EJ, KIM DW, JANG GJ, SONG SH, LEE JI, KIM BM, LEE HJ, HONG HD, CHO CW, KIM HJ. Mass-based metabolomic analysis of *Lactobacillus sakei* and its growth media at different growth phases[J]. *Journal of Microbiology and Biotechnology*, 2017, 27(5): 925-932.
- [30] TOMITA S, SAITO K, NAKAMURA T, SEKIYAMA Y, KIKUCHI J. Rapid discrimination of strain-dependent fermentation characteristics among *Lactobacillus* strains by NMR-based metabolomics of fermented vegetable juice[J]. *PLoS One*, 2017, 12(7): e0182229.
- [31] DONG SJ, LIN XH, LI H. Regulation of *Lactobacillus plantarum* contamination on the carbohydrate and energy related metabolisms of *Saccharomyces cerevisiae* during bioethanol fermentation[J]. *The International Journal of Biochemistry & Cell Biology*, 2015, 68: 33-41.
- [32] ILLEGHEMS K, de VUYST L, WECKX S. Comparative genome analysis of the candidate functional starter culture strains *Lactobacillus fermentum* 222 and *Lactobacillus plantarum* 80 for controlled cocoa bean fermentation processes[J]. *BMC Genomics*, 2015, 16: 766.
- [33] VEGGE CS, JANSEN van RENSBURG MJ, RASMUSSEN JJ, MAIDEN MCJ, JOHNSEN LG, DANIELSEN M, MacINTYRE S, INGMER H, KELLY DJ. Glucose metabolism via the Entner-Doudoroff pathway in *Campylobacter*: a rare trait that enhances survival and promotes biofilm formation in some isolates[J]. *Frontiers in Microbiology*, 2016, 7: 1877.
- [34] HARUTOSHI T. Exopolysaccharides of lactic acid bacteria for food and colon health applications[M]//*Lactic Acid Bacteria-R&D for Food, Health and Livestock Purposes*. IntechOpen: London, UK, 2013.
- [35] ZHANG WP, ZHAO YJ, ZHAO ZW, CHENG X, LI KT. Structural characterization and induced copper stress resistance in rice of exopolysaccharides from *Lactobacillus plantarum* LPC-1[J]. *International Journal of Biological Macromolecules*, 2020, 152: 1077-1088.
- [36] De ANGELIS M, SIRAGUSA S, CAMPANELLA D, di CAGNO R, GOBBETTI M. Comparative proteomic analysis of biofilm and planktonic cells of *Lactobacillus plantarum* DB200[J]. *Proteomics*, 2015, 15(13): 2244-2257.
- [37] RANG J, HE HC, YUAN SQ, TANG JL, LIU ZD, XIA ZY, KHAN TA, HU SB, YU ZQ, HU YB, SUN YJ, HUANG WT, DING XZ, XIA LQ. Deciphering the metabolic pathway difference between *Saccharopolyspora pogona* and *Saccharopolyspora spinosa* by comparative proteomics and metabolomics[J]. *Frontiers in Microbiology*, 2020, 11: 396.
- [38] FILANNINO P, CARDINALI G, RIZZELLO CG, BUCHIN S, de ANGELIS M, GOBBETTI M, di CAGNO R. Metabolic responses of *Lactobacillus plantarum* strains during fermentation and storage of vegetable and fruit juices[J]. *Applied and Environmental Microbiology*, 2014, 80(7): 2206-2215.
- [39] ZHAO HY, LIU LX, PENG S, YUAN L, LI H, WANG H. Heterologous expression of argininosuccinate synthase from *Oenococcus oeni* enhances the acid resistance of *Lactobacillus plantarum*[J]. *Frontiers in Microbiology*, 2019, 10: 1393.
- [40] WANG WW, HE JY, PAN DD, WU Z, GUO YX, ZENG XQ, LIAN LW. Metabolomics analysis of *Lactobacillus plantarum* ATCC 14917 adhesion activity under initial acid and alkali stress[J]. *PLoS One*, 2018, 13(5): e0196231.
- [41] NIEDERDORFER R, BESEMER K, BATTIN TJ, PETER H. Ecological strategies and metabolic trade-offs of complex environmental biofilms[J]. *npj Biofilms and Microbiomes*, 2017, 3: 21.
- [42] SONG XF, WANG QQ, XU X, LIN JW, WANG XR, XUE YT, WU RN, AN YF. Isolation and analysis of salt response of *Lactobacillus plantarum* FS5-5 from *Dajiang*[J]. *Indian Journal of Microbiology*, 2016, 56(4): 451-460.
- [43] BISCHER AP, KOVACS CJ, FAUSTOFERRI RC, JR QUIVEY RG. Disruption of L-rhamnose biosynthesis results in severe growth defects in *Streptococcus mutans*[J]. *Journal of Bacteriology*, 2020, 202(6): e00728-19.
- [44] HSU CY, CAIRNS L, HOBLEY L, ABBOTT J, O'BYRNE C, STANLEY-WALL NR. Genomic differences between *Listeria monocytogenes* EGDe isolates reveal crucial roles for SigB and wall rhamnosylation in biofilm formation[J]. *Journal of Bacteriology*, 2020, 202(7):

- e00692-19.
- [45] LANGE MD, FARMER BD, DECLERCQ AM, PEATMAN E, DECOSTERE A, BECK BH. Sickeningly sweet: L-rhamnose stimulates *Flavobacterium columnare* biofilm formation and virulence[J]. *Journal of Fish Diseases*, 2017, 40(11): 1613-1624.
- [46] XU CT, SHI ZW, SHAO JQ, YU CK, XU ZN. Metabolic engineering of *Lactococcus lactis* for high level accumulation of glutathione and S-adenosyl-L-methionine[J]. *World Journal of Microbiology and Biotechnology*, 2019, 35(12): 185.
- [47] GONG LC, REN C, XU Y. GlnR negatively regulates glutamate-dependent acid resistance in *Lactobacillus brevis*[J]. *Applied and Environmental Microbiology*, 2020, 86(7): e02615-19.
- [48] WU CH, HSUEH YH, KUO JM, LIU SJ. Characterization of a potential probiotic *Lactobacillus brevis* RK03 and efficient production of  $\gamma$ -aminobutyric acid in batch fermentation[J]. *International Journal of Molecular Sciences*, 2018, 19(1): 143.
- [49] SAFONOVA M, GOLOVNYOVA N. Adhesion factors of lactic acid bacteria and bifidobacteria[J]. *Микробные биотехнологии: фундаментальные и прикладные аспекты*, 2021,13:103-118.
- [50] WEN JZ, YU YX, CHEN MQ, CUI L, XIA Q, ZENG XQ, GUO YX, PAN DD, WU Z. Amino acid-derived quorum sensing molecule alanine on the gastrointestinal tract tolerance of the *Lactobacillus* strains in the cocultured fermentation model[J]. *Microbiology Spectrum*, 2022, 10(2): e0083221.
- [51] SCHIUMA G, LARA D, CLEMENT J, NARDUCCI M, RIZZO R. Nicotinamide adenine dinucleotide: the redox sensor in aging-related disorders[J]. *Antioxidants & Redox Signaling*, 2024. DOI:10.1089/ars.2023.0375.
- [52] GE XC, SHI XL, SHI LM, LIU JL, STONE V, KONG FX, KITTEN T, XU P. Involvement of NADH oxidase in biofilm formation in *Streptococcus sanguinis*[J]. *PLoS One*, 2016, 11(3): e0151142.